LAWRENCE
LIVERMORE
NATIONAL
LABORATORY

UCRL-CONF-204087

Simulations of Target Interactions with Pulsed High Energy Solid State Lasers

Charles Boley, Alexander Rubenchik

May 11, 2004

Solid State and Diode Laser Technology Reviews
Albuquerque, NM, United States
June 8, 2004 through June 10, 2004

Simulations of Target Interactions with Pulsed, High-Energy Solid State Lasers

C. D. Boley and A. M. Rubenchik

University of California
Lawrence Livermore National Laboratory
Livermore, CA 94551

In a solid-state heat capacity laser (SSHCL), waste heat is stored in the lasing slabs, minimizing temperature gradients and optical distortions. After the maximum number of pulses is reached, the slabs are cooled or rapidly exchanged with cool slabs. During the past several years, our laboratory at LLNL has built a number of SSHCLs, demonstrating powers beyond 10 kW. In this paper, we model target interactions produced by a 10 kW device (500 J/pulse and 20 Hz), operating at a wavelength of 1.053 μm. The laser contains 9 Nd:glass slabs pumped by flashlamps.

We calculate the interactions of repeated pulses with a steel slab adjacent to a high explosive (TNT), terminating when HE initiation takes place. Our model describes absorption, heat transport, melting, airflow effects, and HE reactions, in two spatial dimensions (cylindrical geometry) and time. The laser-metal interactions of the model have been validated by comparison with coupon experiments at HELSTF, White Sands Missile Range [1,2]. The model employs temperature-dependent material properties (heat capacity, thermal conductivity, and optical absorptivity) based on experiment and/or reasonable extrapolations. The interaction with HE is modeled by adding a term to the heat conduction equation

$$\rho C \, \partial T / \partial t = \nabla \cdot \kappa \nabla T + \rho Q \exp(-E / kT) / \tau,$$

where Q, E, and τ are the heat of decomposition, the activation energy, and the characteristic reaction time, respectively. The exponential term leads to extremely rapid heating once initiation is reached. Vaporization and disassembly, which are outside the scope of the model, then take place. Our simulations terminate when the temperature anywhere within the HE (in practice, near the interface with the steel) suddenly spikes. This occurs shortly after the HE reaches its critical temperature, which depends on the spot size. For our situation this is about 700 C.

Our model allows for airflow past the steel surface. The flow cools the target and also removes the melt layer. The heat transfer coefficient is determined by transport in the turbulent air boundary layer and is taken from wind tunnel experiments. In our regime, at Mach 0.9, it is of order 0.1 W/(cm^2 K). This is insignificant during a pulse but plays a role between pulses. Melt removal is caused by the shear stress produced by the boundary layer. In the simulations, we avoid a complicated hydrodynamical description by simply removing a steel cell (actually an annulus, in cylindrical geometry) when it liquefies. In reality, the shape of the hole would conform to the direction of the wind, and a small melt layer would remain.

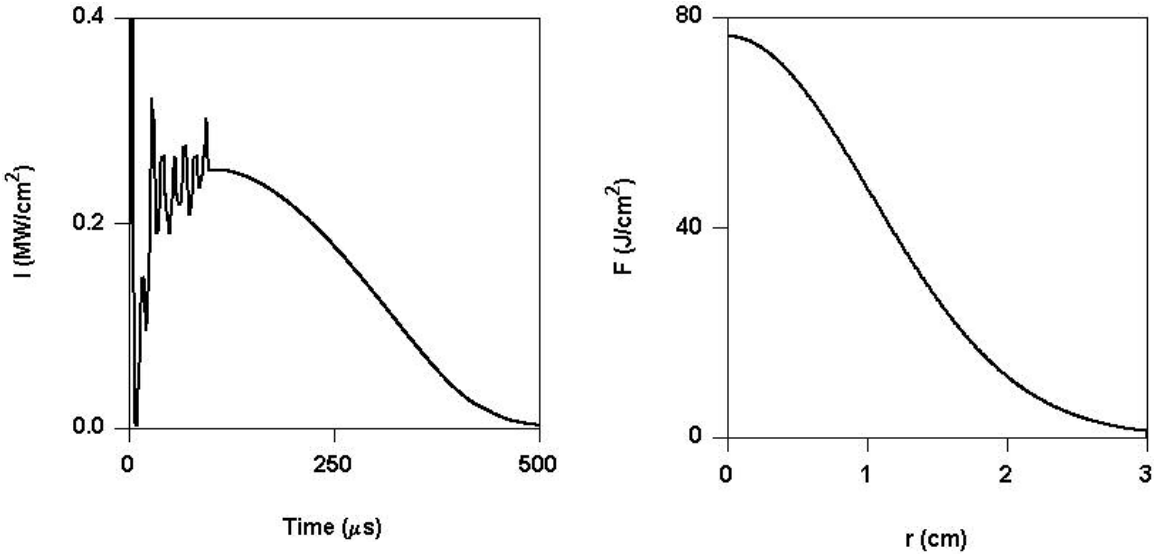

Figure 1. Left: Intensity at beam center. During the first 5 ms, there is a spike of height 2.1 MW/cm^2, accounting for about 7% of the total energy. Right: Radial beam profile.

The beam waveform and transverse profile are shown in Fig. 1. The pulse, as produced by a stable oscillator, has a length somewhat less than 0.5 ms, with considerable structure near the beginning. We work with a Gaussian spatial profile of 1/e radius 1.46 cm. The fluence on this disk is then 75 J/cm^2. The peak intensity of the main pulse is somewhat less than 0.3 MW/cm^2, which produces negligible vaporization or splashing.

During the first pulse, the temperature of the front edge of the steel rises to nearly 1100 C, with or without airflow. Details with airflow are shown in Fig. 2. During the nearly 50-ms interval between pulses, the heat diffuses within the steel and warms the first 100 μm or so of the HE. The interpulse thermal conduction length in steel is about the same as the width of the steel (1 mm). When the second pulse arrives, the temperature on beam center has cooled to approximately 90 C (not shown). Because of the residual heat, successive pulses drive the front edge to successively higher temperatures.

Initiation is found to take place after 11 pulses (0.535 s) without airflow, and after 13 pulses (0.605 s) with airflow. Thus airflow extends the kill time by some 10%. In this case, the temperature of the steel surface, on beam center, reaches a maximum of about 1800 C during the last pulse, as shown in Fig. 2. For initiation purposes, the most important quantity is the maximum temperature of the HE, as a function of time, shown in Fig. 2. This is located on the beam axis, just within the HE. During each pulse cycle before the last, it rises and then levels off. As the figure shows, the onset of reactions in the last cycle is dramatic.

The hot spot in the HE is depicted in Fig. 3. During the 13 pulses, melt removal by airflow leads to a hole of depth about 42 μm on beam center, as also shown in Fig. 3. This is not a dominant effect, since only 4% of the steel thickness is affected.

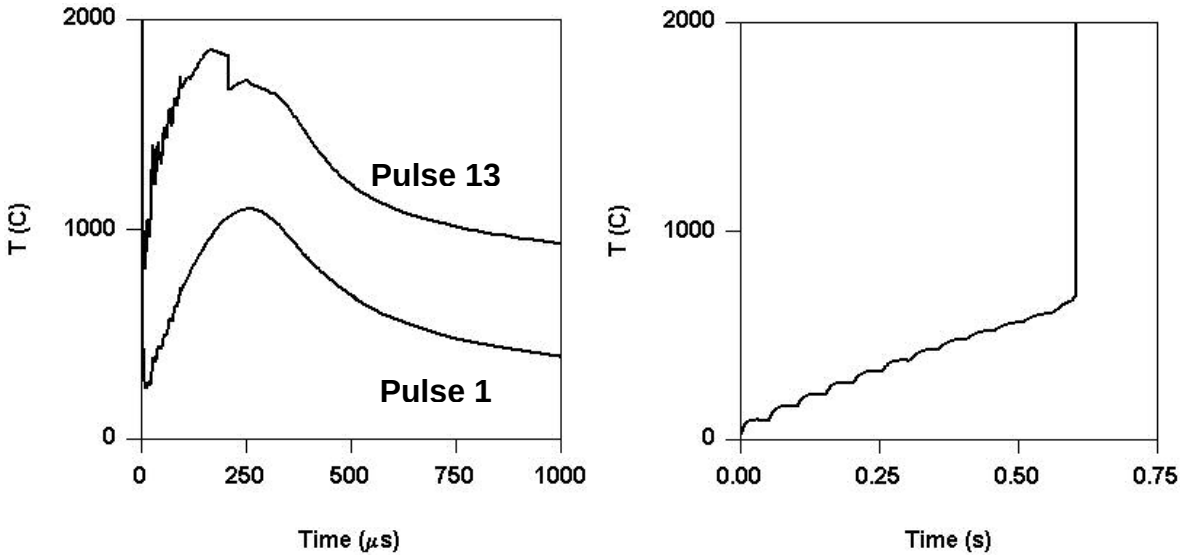

Figure 2. Left: Temperature traces of front edge, radial center, during the first ms of pulses 1 and 13, for the case with airflow. A brief temperature peak caused by the initial intensity spike is not visible on this scale. During pulse 13, the sudden decrease near 200 μs is caused by the removal of a melted cell. Right: Maximum temperature in HE, throughout the 13 pulses. (On the left, time is measured from the beginning of each pulse, while on the right it begins with the first pulse.)

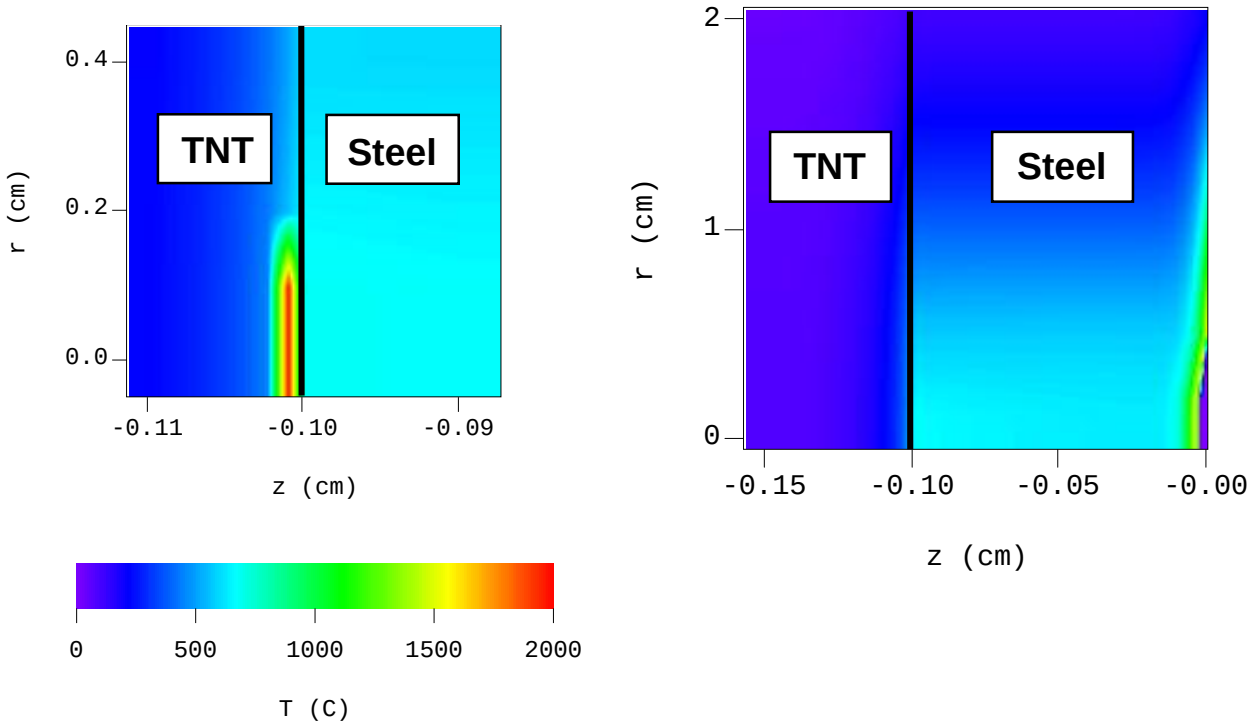

Figure 3. Temperature distribution in the target near the hot spot, at the time of initiation (5 ms into the last pulse cycle), for the case with airflow. Right: Overall temperature distribution in the target at 0.24 ms into last pulse (same color scale). The beam enters from the right. Note the area heated by the beam and the hole (removed melt) at the lower right.

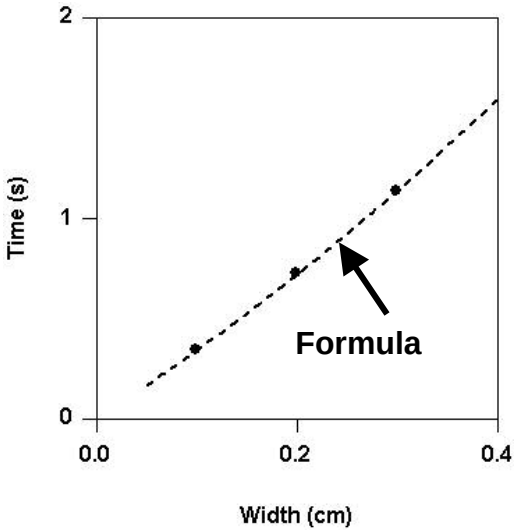

Figure 4. Calculated time for initiation as a function of the width of the steel foil.

Finally, we consider how the time to initiation depends on the thickness of the steel slab. For this purpose, we assume a uniform transverse beam profile irradiating a circular spot of area 5 cm^2. The laser waveform, pulse energy, and repetition rate are the same as before. Airflow is absent. Figure 4 shows the calculated times for widths of 1-3 mm. The time increases somewhat faster than linearly with width. This can be understood as the interplay between (1) the time to reach a given temperature assuming instantaneous conductivity, which increases linearly with width, and (2) the conduction time, which increases quadratically. Also shown is the exact 1D solution for this problem [3], which assumes a constant intensity and constant material properties, appropriately chosen here. In our regime, this solution reduces with good accuracy to

$$t(h) = \rho C h \Delta T / \alpha I + h^2 / 6D,$$

where α is the absorptivity and D is the thermal diffusivity. The two terms correspond to those noted above.

Acknowledgments

We have benefited from many interactions with C. B. Dane, S. N. Fochs, L. A. Hackel, and R. M. Yamamoto. This work was supported by the U.S. Army Space and Missile Defense Command. Work was performed under the auspices of the U.S. Department of Energy by the University of California, Lawrence Livermore National Laboratory, under Contract No. W-7405-ENG-48.

References

[1] C. D. Boley and A. M. Rubenchik, "Modeling of Material Removal by Solid State Heat Capacity Lasers," Proc. 15th Annual Solid State and Diode Laser Technology Review, Albuquerque, NM, June 3-6, 2002.

[2] C. D. Boley and A. M. Rubenchik, "Modeling of High-Energy Pulsed Laser Interactions with Coupons," University of California, UCRL-ID-151857, February 6, 2003.

[3] H. S. Carslaw and J. C. Jaeger, **Conduction of Heat in Solids**, Second Edition, Clarendon Press, 1959, p. 112.